Collisional mechanism of ligand release by Bombyx mori JHBP, a member of the TULIP / Takeout family of lipid transporters.

Stéphane Dupas, Fabrice Neiers, Emma Granon, Erwan Rougeux, Sébastien Dupont, Laurent Beney, François Bousquet, Haq Abdul Shaik, Loïc Briand, Hubert Wojtasek, et al.

Collisional mechanism of ligand release by *Bombyx mori* JHBP, a member of the TULIP / Takeout family of lipid transporters.

Stéphane DUPAS[1], Fabrice NEIERS[1], Emma GRANON[1], Erwan ROUGEUX[1], Sébastien DUPONT[2], Laurent BENEY[2], François BOUSQUET[1], Haq Abdul SHAIK[1], Loic BRIAND[1], Hubert WOJTASEK[3†] and Jean-Philippe CHARLES[1†§].

[1]Université de Bourgogne Franche-Comté, Centre des Sciences du Goût et de l'Alimentation, AgroSup Dijon, UMR 6265 CNRS, UMR 1324 INRA, 6, Bd Gabriel, F-21000, Dijon, France.

[2]Université de Bourgogne Franche-Comté, AgroSup Dijon, PAM UMR A 02.102, F-21000, Dijon, France.

[3]Institute of Chemistry, Opole University, Ul. Oleska 48, 45-052 Opole, Poland.
Hubert.Wojtasek@uni.opole.pl.

[†] These authors share senior authorship

[§] Corresponding author Jean-philippe.charles@u-bourgogne.fr

ABSTRACT:

Juvenile hormones (JHs) regulate important processes in insects, such as postembryonic development and reproduction. In the hemolymph of Lepidoptera, these lipophilic sesquiterpenic hormones are transported from their site of synthesis to target tissues by high affinity carriers, the juvenile hormone binding proteins (JHBPs). Lepidopteran JHBPs belong to a recently uncovered, yet very ancient family of proteins sharing a common lipid fold (TULIP domain) and involved in shuttling various lipid ligands. One important, but poorly understood aspect of JHs action, is the mechanism of hormone transfer to or through the plasma membranes of target cells. Since many membrane-active peptides and proteins, such as the pore-forming bacterial toxins, are activated by low pH or interaction with phospholipid membranes, we have examined the effect of these factors on JH binding by JHBPs. The affinity of *Bombyx mori* and *Manduca sexta* JHBPs for JH III was determined by the DCC assay, equilibrium dialysis, and isothermal titration calorimetry, and found to be greatly reduced at low pH, in agreement with previous observations. Loss of binding was accompanied by changes in fluorescence and near-UV CD spectra, indicating significant changes in protein structure in the environment of aromatic residues. The apparent dissociation rate constant (k_{off}) of the JHBP-JH III complex was greater at acidic pH, suggesting that low pH favors ligand release by opening of the binding pocket. The affinity of recombinant *B. mori* JHBP (r*Bm*JHBP) was also decreased in the presence of anionic phospholipid vesicles. Measurements of steady-state fluorescence anisotropy with the lipophilic probe TMA-DPH demonstrated that r*Bm*JHBP specifically interacts with anionic membranes. These results suggest the existence of a collisional mechanism for ligand release that may be important for delivery of JHs to the target cells, and could be relevant to the function of related members of this emerging family of lipid-transport proteins.

Keywords:

Juvenile Hormone
JHBP
Bombyx mori
Manduca sexta
TULIP domain
Takeout-like proteins

1. Introduction

Juvenile hormones (JHs) regulate important processes in insects, such as postembryonic development and reproduction (Goodman and Cusson, 2012; Jindra et al., 2015). In the hemolymph of Lepidoptera, JHs are transported from their site of synthesis (the *corpora allata*) to target tissues by high affinity carriers, the juvenile hormone binding proteins (JHBPs). It is believed that these proteins protect the hormones from degradation and non-specific adsorption to lipophilic depots (Goodman, 1990; Koeppe and Kovalick, 1986).

For a long time, the details of JHBP-JH interactions have remained elusive. The X-ray structure of apoJHBP was first determined for the protein from *Galleria mellonella* (Kolodziejczyk et al., 2008). The structure consists of a long α-helix surrounded by a twisted, anti-parallel ß-sheet with two cavities forming potential binding sites at the opposite ends of the molecule (Figure S1). It closely resembles the structure of several other lipid binding proteins, such as the Takeout 1 protein of the moth

Epiphyas postvittana (Hamiaux et al., 2013; Hamiaux et al., 2009), as well as the mammalian bactericidal/permeability increasing protein (BPI) (Beamer et al., 1997) and the cholesteryl ester transfer protein (CETP) (Qiu et al., 2007). Phylogenetic analyses have shown that these proteins and many others, including plant proteins, share one or two copies of an ancestral TULIP lipid binding motif (Tubular Lipid binding), which allows lipid transport, as well as interaction with phospholipids at the surface of membranes or lipoproteins (Alva and Lupas, 2016; Wong and Levine, 2017). Although very ancient and therefore likely playing fundamental functions in lipid trafficking for most eukaryotes and prokaryotes, the functions of the members of this emerging family are mostly known from studies in mammals. In invertebrates, the TULIP domain proteins Takeout and Takeout-related proteins have been involved in various processes (courtship behavior, feeding, aging, JH transport, perception (Fujikawa et al., 2006; Galikova and Flatt, 2010; Lazareva et al., 2007; Meunier et al., 2007; Sarov-Blat et al., 2000; Yoshizawa et al., 2011)). Lepidopteran JHBPs appear to constitute a subclass of the Takeout proteins, characterized by the presence of a conserved disulfide bridge dividing the large internal hydrophobic cavity into two smaller ligand binding pockets (Hamiaux et al., 2013; Hamiaux et al., 2009; Kolodziejczyk et al., 2008; Kolodziejczyk et al., 2001). To this day, JHBPs are the only members with well characterized endogenous ligands.

The structure of JHBP from *Bombyx mori* with a bound hormone was solved by both X-ray diffraction and NMR spectroscopy (Suzuki et al., 2011). This study revealed that ligand uptake and release are accompanied by substantial conformational changes of the protein, in agreement with earlier findings on *G. mellonella* JHBP (Krzyzanowska et al., 1998; Wieczorek and Kochman, 1991). It was shown that the N-terminal helix functions as a gate, which closes upon ligand binding. In the apo form of the protein in the crystalline state, the gate is open, allowing access of the ligand to the binding site. In solution, the gate of the apoJHBP is highly mobile and the protein exists in multiple conformations, including the gate-open conformation, seen in the crystalline state, and the gate-closed conformation similar to the ligand-bound form. This flexibility of the gate in the apo-JHBP disappears upon JH-binding. Based on these structural changes a mechanism of JH delivery to target cells has been proposed ((Suzuki et al., 2011), Figure S1).

Release of a hydrophobic ligand from a complex with a binding protein has been previously demonstrated for a number of proteins. *B. mori* pheromone-binding protein (PBP) (Horst et al., 2001) binds its ligand only at neutral and basic pH, whereas low pH induces the formation of an additional α-helix (helix 7), which fills the binding pocket and prevents ligand binding. Analysis by CD and fluorescence spectroscopy has demonstrated that structural changes, very similar to those evoked by low pH, were also induced by phospholipid vesicles (Wojtasek and Leal, 1999), and it was therefore hypothesized that pheromone release could be triggered by phospholipid membranes on the surface of olfactory neurons, thus providing a mechanism of ligand delivery to target cells.

Evidence for pH-induced ligand release has also been shown for several other hydrophobic ligand binding proteins, including serum retinol binding protein (Ptitsyn et al., 1993) and tear lipocalin (Gasymov et al., 2004). More generally, acidic pH and interaction with phospholipidic membranes are two common triggers for membrane-active proteins, such as pore-forming bacterial toxins or viral fusion proteins (Butko et al., 1994; Harrison, 2015; Jiang and London, 1990; London, 1992; Menestrina et al., 1989).

We have investigated the effects of pH and phospholipid membranes on ligand binding by *B. mori* and *Manduca sexta* JHBPs by several methods. We show that acidic pH substantially reduces JHBP affinity for JH III, apparently increasing its k_{off}, which suggests that low pH favors ligand release, presumably by keeping the protein in the open conformation. We also report that JH III binding is diminished in the presence of anionic phospholipid liposomes, and that *B. mori* JHBP significantly interacts with these membranes. Taken together, the results support a collisional model of ligand release mechanism triggered by specific electrostatic and hydrophobic interactions on the surface of the plasma membrane of target cells.

2. Material and methods

2.1. Purification of native JHBP

Hemolymph JHBP from *B. mori* was purified using a modification of a published procedure (Kurata et al., 1994). The hemolymph was collected from fifth instar day 4 larvae into Falcon tubes on ice, frozen in liquid nitrogen and lyophilized. The lyophilizate was dissolved in 0.5 mM phenylthiourea in water before purification, centrifuged for 10 min at 10000 g and dialyzed against 20 mM Tris-HCl, pH 7.5 overnight at 4 °C. The dialyzed sample was applied to a DEAE-Sepharose (DFF-100, Sigma-Aldrich) column and the proteins were eluted with a stepwise gradient of 50-300 mM NaCl in 20 mM Tris-HCl, pH 7.5. Fractions containing JHBP were pooled, mixed with an equal volume of 2 M ammonium sulfate and applied to a Phenyl-Sepharose (Fast Flow, high substitution, GE HealthCare) column. Proteins were eluted with a stepwise gradient of 0.75-0.1 M ammonium sulfate in 20 mM Tris-HCl, pH 7.5 and then water. Fractions containing JHBP were pooled again and applied to a hydroxyapatite (Ceramic Hydroxyapatite Type I, BioRad) column. Proteins were eluted with a stepwise gradient of 10-300 mM sodium phosphate buffer, pH 6.8. Fractions from each purification step were analyzed by SDS-PAGE and DCC binding assay (Figure S2). This protein preparation of native *B. mori* JHBP (n*Bm*JHBP) was used for initial binding studies (Figure 1), testing the effect of ionic strength (Figure S6), and estimation of k_{off} (Figures 5, S8). Other experiments were performed with recombinant *B. mori* (r*Bm*JHBP, see below).

2.2. Expression of recombinant JHBPs

B. mori larvae were reared on mulberry leaves under natural daylight conditions. Fat body was isolated from fifth instar day 5 larvae, frozen in liquid nitrogen and stored at -70 °C. Total RNA was isolated with the single phenol-chloroform-isothiocyanate extraction method (Chomczynski and Sacchi, 1987), and mRNA was isolated with the PolyATtract mRNA Isolation system III (Promega). The cDNA was synthesized with AMV reverse transcriptase and a primer corresponding to the mRNA fragment encoding the C-terminus of JHBP. The reverse transcription reaction mixture was used directly for PCR reactions with Pfu DNA polymerase and primers designed based on the published *B. mori* JHBP cDNA sequence (Vermunt et al., 2001): JHBPBmF (5'-GCAGAATTCCCATGGGAGATGGAGATGCTCTT) and JHBP-BMX-rev2 (5'-CGGTGAATTCTTAATTAAGATTTTCG), and the product coding the mature form of the protein (starting with Asp19 immediately after the signal peptide excision site (Vermunt et al., 2001) was ligated at the *Eco*RI site of pGEM™-T Easy Vector (Promega). An insert in the right orientation was excised with *Eco*RI and *Nco*I, and ligated at the *Eco*RI and *Nco*I sites of Pet-22b vector (Novagen, Merck) in frame with the pelB leader, allowing periplasmic localization. We found 28 nucleotides differing from the original published sequence (Vermunt et al., 2001), among which 10 yielded amino acid substitutions. These differences likely stem from the natural allelic diversity amongst *B. mori* strains (Figure S3). A cDNA kindly provided by W.G. Goodman (University of Wisconsin-Madison), was used as a template to amplify the sequence encoding *M. sexta* JHBP with primers JHBP-Manduca-fw (5'-ATATCCATGGGAGATCAAGGGGCACT) and JHBP-Manduca-rev (5'-CGCTGAATTCAAAATTAATTAACATCC). The product coding the mature form of the protein (starting with Asp19 immediately after the signal peptide excision site (Touhara et al., 1993) was fused in frame with the pelB leader in Pet-22b. As we failed to obtain soluble protein with the pelB leader system, the sequence coding for pelB was removed by digesting pET-22b (+) with *Nde*I and *Mls*I, the ends were polished with Klenow, and ligated to yield pET-22b-(minus)-pelB plasmids, encoding the mature forms with two extra residues (Met1 and Gly2) at the amino-terminus. Shuffle bacteria (New England Biolabs) were transformed with either *B. mori or M. sexta* Pet-22b-(minus)-pelB JHBP plasmid, grown in the presence of 0.5% glucose and protein expression was induced by IPTG. Bacterial pellets were lysed for 15 min at 30 °C in a lysis buffer (25 mM Tris-HCl, pH 8.0, 200 mM NaCl, 100 µg/mL lysozyme, and proteases inhibitors), sonicated on ice, and centrifuged for 10 min at 12000 g. Recombinant JHBPs from *M. sexta* (r*Ms*JHBP) and *B. mori* (r*Bm*JHBP) were purified from bacterial lysates essentially as described above for the native protein from *B. mori* (Figure S2).

2.3. Ligand Binding Assays

The DCC (Dextran Coated Charcoal) assay was performed essentially as described previously (Touhara et al., 1993). Unless indicated otherwise, the continuous buffer system of McIlvaine

composed of citrate and phosphate was used to explore the binding for various pH values (McIlvaine, 1921). For typical DCC assays, JHBP (50-300 nM) was diluted in a final volume of 100 µL of buffer containing a JH esterase inhibitor (OTFP: 3-octylthio-1,1,1-trifluoro-2-propanone, a kind gift of B.D. Hammock (University of California) at a final concentration of 1 µM, and about 10000 dpm [^{3}H]-JH III (~ 20 Ci/mmol, Perkin-Elmer). After incubation at room temperature (ca. 20 °C) for one hour in a 6 x 50 mm borosilicate glass tube (Kimble-Chase, # 73500-650) precoated with a 10 % polyethylene glycol solution ((Goodman et al., 1976), Sigma # 95172), 20 µL of a DCC slurry (5% (w/v) activated charcoal (Norit A, ACROS Organics # 134342500), 1 % (w/v) Dextran (Sigma # D4751), 1.5 mM EDTA) was added and the mixture was gently mixed by vortexing for about 2 s. After a 30 s incubation, the tubes were centrifuged (ca. 10000 g, 2 min), and the radioactivity of a 50 µL aliquot of the supernatant was measured in a scintillation counter to estimate the amount of bound [^{3}H]-JH III. In these conditions, 10-50 % of [^{3}H]-JH III was bound by JHBP. For dialysis assays, 70 µL of a buffer containing about 70000 dpm of [^{3}H]-JH III was loaded into each chamber of a disposable dialysis device with a 10 kDa MW cut-off (Harvard Apparatus, Holliston, MA, U.S.A.). Proteins (1-5 µg of purified JHBP or bovine serum albumin (BSA) used as a control), were added to one chamber of the device. After overnight incubation at 4 °C, an aliquot of each chamber was counted in a scintillation counter, and the percentage of bound ligand was determined. For experiments involving lipid membranes, varying amounts (5-600 µg) of liposomes were added to the chamber of a dialysis device with or without JHBP.

2.4. Isothermal titration calorimetry

Isothermal titration calorimetry (ITC) experiments were carried out at 293 K and 298 K using a VP–ITC microcalorimeter (GE Healthcare). r*Bm*JHBP was dialyzed against 100 mM sodium phosphate buffer, pH 7.0, or 100 mM sodium acetate buffer, pH 4.5. Solutions of JH III were prepared in the same buffer as used for dialysis. The titration sequence included a single 3 µL injection followed by 25 injections of 10 µL of ligand solution, with 210 s intervals between injections. Measurements were performed for 5 µM protein with 70 µM ligand, or 2.5 µM protein with 35 µM ligand. The OriginLab software (GE Healthcare) was used to fit the raw data using a single binding-site model. For the analysis the data points obtained after the first 3 µL injection were discarded. The experiments were performed 3 times for each ligand and protein concentrations indicated, and the dissociation constants (K_d) were calculated.

2.5. Circular dichroism

Near UV CD spectra were recorded between 250 and 320 nm in a JASCO J-815 spectropolarimeter at 20 °C, using a 1 cm path length quartz cell (Hellma). r*Bm*JHBP (25 µM) was dissolved in McIlvaine buffer at pH 3.5, 4.5, 5.5, 6.5 or 7.5. Data were averaged over 10 accumulated scans recorded at 1 nm intervals with a 50 nm/min scan speed. The spectra were corrected for buffer contributions and converted to molar ellipticity in deg•cm^2•dmol^{-1}.

2.6. Tryptophan fluorescence spectroscopy

The intrinsic fluorescence of r*Bm*JHBP was measured with a Cary Eclipse spectrofluorometer (Varian Instruments) at 20 °C, in a 2 mL quartz cuvette with a 1 cm path length equipped with a magnetic stirrer. The effect of ligand addition was examined using r*Bm*JHBP at 10 µM final concentration before and after 15 min equilibration with JH III at various concentrations (1.18, 2.32, 3.42, 6.5, 11.87 and 20.25 µM) in 100 mM sodium phosphate buffer, pH 7.0. The proteins were excited at 293 nm and emission spectra were recorded from 320 to 450 nm with a 10 nm bandwidth for both emission and excitation. The results were corrected for the dilution due to the addition of different volumes of JH III solution. For each ligand concentration, two or three spectra were recorded and averaged.

To study pH-dependent changes in fluorescence, a small volume of the concentrated r*Bm*JHBP protein (28 µL), was added to a large volume of McIlvaine buffer (972 µL) at different pH values (4.5, 5.5, 6.5, 7.0, 7.5), thus ensuring a minor pH change of the final 10 µM protein solution.

Fluorescence was recorded as described above. Three independent measurements were performed for each pH value and the spectra were averaged.

2.7. Light scattering

The size and homogeneity of r*Bm*JHBP at neutral and acidic pH in McIlvaine buffers were examined by light scattering using a Zetasizer Nano S apparatus (Malvern, U.K.).

2.8. Liposome preparation

Solutions of lipids (DMPG (1,2-dimyristoyl-*sn*-glycero-3-phosphoglycerol, Sigma #43096), DMPC (1,2-dimyristoyl-*sn*-glycero-3-phosphocholine, Sigma #P-2663), or a 1:1 mixture of both) at a 10 mg/mL concentration in chloroform were evaporated, first by heating at 45 °C under a nitrogen stream, then for further 2-6 h with a centrifugal evaporator (Speedvac). The lipids were suspended in water (10 mg/ml), aliquoted and stored at -20 °C. Unilamellar liposomes were obtained by extrusion of the phospholipid suspension through a 100 nm pore size polycarbonate filter (Liposofast, Avestin), at 37 °C. The final amount of phospholipid was verified by gas chromatography, and the quality (size and distribution) of the unilamellar liposomes was verified by light scattering.

2.9. Determination of fluidity of DMPG liposomes

Membrane fluidity of DMPG liposomes was assessed by the steady-state fluorescence polarization of 1-(4-trimethylammoniumphenyl)-6-phenyl-1,3,5-hexatriene *p*-toluenesulfonate (TMA-DPH) (Sigma Aldrich). The concentration of liposomal preparations was adjusted to 10 mg/mL in McIlvaine buffer, pH 7.0. Protein solutions (r*Bm*JHBP, heat-denatured r*Bm*JHBP or BSA) were prepared in 1 mM Tris-HCl, pH 7.0, at a concentration of ca. 40 nM. TMA-DPH was prepared as a 1 mM stock solution in tetrahydrofuran (THF). The liposomal preparations (30 µL) were transferred to a cuvette containing 2970 µL of buffer (1 mM Tris-HCl, pH 7.5) and labeled with TMA-DPH by addition of 4 µL of the stock solution. The suspension was stirred for 15 min at 35 °C to allow the probe to insert in the lipid bilayer. For the study of the effect of the proteins on liposome fluidity, 50 µL of protein solutions were added to the cuvette before labeling with TMA-DPH. Anisotropy measurements were performed in a range of temperatures between 35 °C and 11 °C, with a Fluorolog-3 spectrometer (Jobin-Yvon, Horiba Group, USA), using T-format fluorescence polarizers, equipped with a thermoelectric Peltier junction. The excitation and emission wavelengths were 360 nm (5 nm bandwidth) and 431 nm (5 nm bandwidth), respectively. Steady-state fluorescence anisotropy (r) was calculated as follows: $r = (I_{vv} — GI_{vh})/(I_{vv} + 2\,GI_{vh})$, where I stands for the fluorescence intensity and the first and second subscripts refer to the setting of the excitation and emission polarizers, respectively. $G = I_{hv}/I_{hh}$ is a correction factor for the monochromator's transmission efficiency for vertically (v) and horizontally (h) polarized light.

2.10. Statistical analyzes

All analyses (Student's test, curve fittings, determination of pH_{50}, determination of the temperature of phase transition) were performed with Graphpad Prism version 5.0d for Mac OS X (GraphPad Software, La Jolla, California USA).

3. Results

3.1. Low pH reduces affinity of native and recombinant lepidopteran JHBPs for JH III

A sharp decrease of binding affinity of Lepidopteran JHBP in the low pH range was first discovered for the *G. mellonella* protein (Ozyhar and Kochman, 1987), and a similar correlation was later reported for the recombinant *B. mori* JHBP (Suzuki et al., 2011). We have examined the affinity of the native JHBP from *B. mori*, and recombinant proteins from *B. mori* and *M. sexta* with the Dextran Coated Charcoal (DCC) assay, and also observed a steep decrease of affinity at low pH in all

three cases, with a 50% reduction of binding in the pH range between 4 and 5.5 (Figure 1A). The native proteins were more sensitive to hydrogen ion concentration (pH_{50} values for n*Bm*JHBP and n*Gm*JHBP (inferred from data in (Ozyhar and Kochman, 1987)) were 5.08 and 5.45, respectively), than the recombinant proteins from *B. mori* and *M. sexta* (pH_{50} values were 4.18 and 4.67, respectively). The cause of the lower sensitivity of the recombinant proteins is unclear. The effect of low pH on n*Bm*JHBP, r*Bm*JHBP and r*Ms*JHBP was also examined using a dialysis assay (Figure 1B). The results showed a significant (two- to four-fold, $p<0.001$, Student's t test, n=3) reduction of binding at pH 4, when compared to pH 7. In addition, the relative sensitivity of the three proteins was the same as found with the DCC assay (Figure 1B): n*Bm*JHBP was the most sensitive, whereas r*Bm*JHBP showed only a *ca*. twofold reduction in affinity at pH 4 in this assay.

The dissociation constant (K_d) of the recombinant *B. mori* JHBP for JH III was then determined at pH 4.5 and pH 7.0 by isothermal titration calorimetry (Figure 1C, D). Consistently with the above data, the K_d is increased at acidic pH. Interestingly, increasing the temperature to 25 °C had opposite effects at pH 4.5 and pH 7, as the K_d was increased at pH 4.5, but lowered at pH 7. This difference of dependence of the K_d on temperature may reflect the existence of distinct conformations of r*Bm*JHBP at acidic and neutral pH (Vega et al., 2016). The K_d measured at 25 °C and pH 7 (37 nM) is similar to the K_d for JH II reported for a baculovirus-produced *M. sexta* JHBP (42 nM, (Touhara et al., 1993)), but much lower than the Kd for JH III reported earlier for a *B. mori* JHBP expressed in *E. coli* (450 nM, (Vermunt et al., 2001)). The K_ds reported in this study are, however, higher than those reported for enantiomerically-pure JH III and native *M. sexta* JHBP which were determined by equilibrium dialysis (1.86 nM, (Park et al., 1993)). These differences likely result from the varying conditions used in the different studies, notably the procedures for protein production and/or purification, the nature and purity of the ligands, and the methods used for binding assays (Park et al., 1993)). The effect of low pH cannot be accounted for by pH-dependent solubility of the ligand or ligand breakdown (such as through hydrolysis of the epoxide ring by nucleophilic attack at low pH (Figure S4)). Moreover, light scattering analysis showed that the apparent size and aggregation of recombinant r*Bm*JHBP were essentially the same at acidic and neutral pH (Figure S5).

Since the ionic strength of McIlvaine buffers changes with pH (0.157 M at pH 4, and 0.427 M at pH 7, (Elving et al., 1956)), we were also concerned that this factor may contribute to changes in binding. However, binding experiments in the presence of 0-0.6 M NaCl showed that the binding affinity decreases with increasing ionic strength (Figure S6). Therefore, reduced binding at low pH can likely be attributed to increased proton concentration, rather than reduced ionic strength.

3.2. Reduced JH III binding at low pH is reversible

We next asked whether this effect of low pH on JHBP affinity could be reversed. When n*Bm*JHBP was first allowed to bind JH at neutral pH and reach equilibrium, adjusting the pH to a value of 4 was sufficient to reduce dramatically the amount of bound JH. Conversely, after one hour incubation at pH 4, full binding activity could be recovered by adjusting the pH back to neutrality (Figure 2).

3.3. Effect of pH on JHBP structure

We next tested the hypothesis that reduced binding at acidic pH could be evoked by a switch from the closed to the open conformation, as proposed by Suzuki and colleagues (Figure S1) (Suzuki et al., 2011). Far and near UV circular dichroism (CD) analyses were performed to examine if the structure of JHBP is different at acidic and neutral pH. For these and further experiments r*Bm*JHBP was used, except as indicated. Little change was observed in far UV CD spectra (Figure S7), suggesting that the secondary structure of r*Bm*JHBP is essentially unchanged at these two pH values, consistently with the open and closed forms determined by NMR (Suzuki et al., 2011). These data show in addition that r*Bm*JHBP is well structured at both pHs.

In contrast, however, near UV CD spectra taken at several pH values showed significant differences, indicating changes in the tertiary structure of the protein (Figure 3). We also obtained fluorescence spectra, taking advantage of the fact that *B. mori* JHBP contains a single tryptophan residue (Trp38) (Vermunt et al., 2001), in the loop forming the gatepost for the gate-forming α1 helix

near the entrance of the ligand binding pocket (Figure 4, Figure S1, (Suzuki et al., 2011)). At neutral pH, ligand binding induces a change in the environment of Trp38, as evidenced by a significant drop of fluorescence emission at 293 nm with JH III concentrations ranging from about 1 to 20 µM (Figure 4A). This result shows that the environment of Trp38 changes, and is consistent with the fact that the nearby α1 helix, which forms the "gate" of the ligand binding pocket, undergoes a major change of position upon ligand binding (Figure S1, (Suzuki et al., 2011)). Importantly, lowering the pH also strongly affected fluorescence intensity (Figure 4B). The fact that a drop in fluorescence emission is observed in both experiments is not paradoxical, because the fluorescence of tryptophan is known to be exquisitely sensitive to changes in the local environment (Hellmann and Schneider, 2019; Royer, 2006), and the mere presence (Figure 4A) or absence (Figure 4B) of ligand, may have strong and hardly predictable effects.

Although we cannot exclude that the change in fluorescence seen with decreasing pH is partly due to the protonation of His206, which is bound to Trp38 by π-π stacking interactions (Suzuki et al., 2011), this observation, together with UV CD spectra, suggests that at acidic pH, r*Bm*JHBP undergoes a significant change in tertiary structure that may involve the switch of the α1 helix into the " open " conformation, and hence trigger ligand release.

3.4. Binding kinetics

Considering the hypothesis that the reduced binding observed at low pH (Figure 1), or at high ionic strength (Figure S6), results from the opening of the gate-forming α1 helix, we expected that in both conditions the dissociation rate constant (k_{off}) of the n*Bm*JHBP-JH III complex would be increased. To address this point, we attempted to estimate k_{off} using a modified DCC assay. As shown in Figure 5A, the estimated k_{off} of the complex was unchanged at high ionic strength, suggesting that low JH binding in this condition is caused by reduced access of JH III to the binding pocket, rather than by increased ligand release. In contrast, at acidic pH, the k_{off} appeared roughly three times greater than at neutral pH (Figure 5B). This result suggests that a high proton concentration may contribute to ligand release by n*Bm*JHBP. The absolute values for k_{off} measured here should be considered as preliminary and rough estimates (since protein loss was evident for longer incubation times in this assay (Figure S8)). The k_{off} values determined at pH 7 in this study (ca. 0.033 s^{-1}, Figure 5) are similar to those measured for the native *M. sexta* JHBP-JH III complex by two different approaches (0.0525 s^{-1} and 0.0357 s^{-1}, (Park et al., 1993)), but must be confirmed in future experiments with a dedicated and accurate method (such as stop-flow spectroscopy). Together with the observation that low pH provokes a change in fluorescence intensity (Figure 4B), however, these results are consistent with the hypothesis that low pH contributes to a switch from the "closed" to the "open" conformation of the α1 helix.

3.5. Interaction of JHBP with lipid vesicles

It was previously shown that if the dielectric constant of a binding mixture is increased by adjusting the solution to a final concentration of 30 % ethanol, thereby mimicking the hydrophobic environment of the cell membranes, JH III was released from JHBP (Suzuki et al., 2011). We have therefore decided to examine if ligand binding by r*Bm*JHBP is modified in the presence of phospholipid membranes. Unilamellar phospholipid vesicles composed of either pure anionic 1,2-dimyristoyl-*sn*-glycero-3-phosphoglycerol (DMPG), or a 1:1 mixture of DMPG and 1,2-dimyristoyl-*sn*-glycero-3-phosphocholine (DMPC, a zwitterionic phospholipid) were prepared, and their influence on JH binding was assessed by a dialysis assay (Figure 6). JHs are lipophilic hormones, and were shown earlier to partition into phospholipid membranes (Barber et al., 1981). Therefore, as expected, DMPG liposomes loaded in one chamber of a dialysis device bound [^{3}H]-JH III in a dose-dependent manner from 5 µg to 200 µg per assay, with a plateau at about 70% bound ligand (Figure 6, white columns). In this dialysis assay, r*Bm*JHBP alone showed robust binding to [^{3}H]-JH III at neutral pH (Figure 6, black column). However, when JHBP was incubated with the ligand in the presence of DMPG vesicles at an amount equal to or greater than 40 µg, the percentage of bound [^{3}H]-JH III was significantly lower than when r*Bm*JHBP was incubated alone (Figure 6, striped columns). This result therefore suggests that interaction with DMPG liposomes prevents binding of JH III by r*Bm*JHBP. The

anionic nature of the phospholipid was apparently important for this effect, since even a high (600 µg) amount of liposomes composed of a 1:1 mixture of the anionic DMPG and zwitterionic DMPC, was barely sufficient to significantly reduce JH III binding by r*Bm*JHBP (Figure 6, grey columns).

To examine the effect of anionic phospholipids more closely, the interaction of r*Bm*JHBP with DMPG liposomes was analyzed by a steady-state fluorescence polarization method ((Borenstain and Barenholz, 1993), Figure 7). The fluorescence anisotropy of the TMA-DPH probe embedded in lipid membranes is a measure of the motional order within the headgroup region of the phospholipids, as far down as C_8-C_{10} (Prendergast et al., 1981). DMPG liposomes were incubated first with the hydrophobic fluorescent probe TMA-DPH alone. The decreasing slope of TMA-DPH fluorescence anisotropy with temperature was relatively shallow, consistently with earlier observations ((Lamy-Freund and Riske, 2003); Figure 7: liposomes alone). The shape of the temperature-dependent anisotropy curve was significantly different in the presence of r*Bm*JHBP (Figure 7: r*Bm*JHBP). Below 20 °C, the motion of acyl chains was increased, while membrane phospholipids were stabilized between 20 °C and 27 °C. Importantly, neither BSA nor heat-denatured r*Bm*JHBP had an effect on TMA-DPH fluorescence. These results indicate that r*Bm*JHBP strongly interacts with DMPG membranes at neutral pH, and that this interaction requires a proper folding of the protein.

4. Discussion

More than three decades ago, in their study of *G. mellonella* JHBP, Ozyhar and Kochman reported a steep decrease in its JH binding activity below pH 7, and proposed that this peculiar activity profile may be shared by JHBPs from other species ((Ozyhar and Kochman, 1987), Figure 1). A similar pH-sensitivity was later observed for a recombinant *B. mori* JHBP (Suzuki et al., 2011). We report here that the native JHBP purified from larval *B. mori* hemolymph, as well as recombinant JHBPs from this species and *M. sexta*, share indeed with their *G. mellonella* homologue a similar sensitivity profile at low pH (Figure 1).

We think that this conserved feature may hint to the existence of a biologically relevant ligand release mechanism involving the switch of the gate-forming α1 helix, as proposed by Suzuki and coworkers (Figure S1, (Suzuki et al., 2011)). This hypothesis is supported by UV fluorescence and circular dichroism spectrometry, as well as light scattering data, showing that the secondary structure of *B. mori* JHBP is very similar at acidic and neutral pH, whereas in contrast, significant changes in tertiary structure are observed, consistently with a conformational switch of the α1 helix (Figures 3, S5, S7).

Our fluorescence spectrometry data indicate that low pH also strongly influences the fluorescence intensity of r*Bm*JHBP (Figure 4B), which likely reflects a significant change occurring in the environment of Trp 38, located in the "gatepost" of *B. mori* JHBP (Figure S1). This result would be expected if the α1 helix switches to the closed conformation upon ligand binding, and is consistent with the apparent increase of k_{off} of the n*Bm*JHBP-JH III complex (Figure 5). In their NMR studies, Suzuki and colleagues observed that there were only small differences in chemical shifts for most residues when JHBP was incubated at pH 4 or pH 6, and that the intermolecular NOEs between JH III and JHBP were conserved in both conditions, indicating that JH III was bound at acidic pH. Although these results may appear in contradiction with ours, this discrepancy may be explained by the high (0.6-1 mM) concentrations of JHBP and ligand applied in NMR experiments (Suzuki et al., 2011). Considering the K_d values determined in this study (Figure 1D), and the generally accepted maximal concentration range for juvenile hormones in aqueous solutions (30 to 50 µM (Kramer et al., 1974)), the law of mass action predicts a high fractional JHBP occupancy (> 90%) at both neutral and acidic pH at concentrations applied in NMR experiments.

The TULIP superfamily of LTPs, to which JHBP belongs, has recently been recognized as very ancient, since it is present in a wide range of animal, fungal, algal, and plant cells, as well as in prokaryotic cells (Alva and Lupas, 2016; Wong and Levine, 2017). TULIP domain proteins are involved in a variety of processes related to lipid shuttling, either between membrane compartments or lipoprotein particles, such as HDL and LDL. In vertebrates, the plasma phospholipid transport protein (PLTP) and the cholesteryl-ester transfer protein (CETP), both harboring two TULIP domains, have well known functions in neutral lipid and phospholipid transfer between lipoprotein particles (Masson et al., 2009; Tzotzas et al., 2009). Although the details of the molecular mechanisms of docking and

lipid transfer of CETP and PLTP to lipoproteins are still debated, it is now well established that CETP interacts strongly with the outer phospholipid layer of lipoproteins (Lauer et al., 2016; Qiu et al., 2007; Zhang et al., 2012). Its N-terminal end penetrates ca. 50 Å into HDL particles, thus fully crossing the 18-27 Å phospholipid layer. Interestingly, shallow penetration into liposomes has also been observed (Charles and Kane, 2012), and CETP can efficiently load lipids from liposomes and deliver them to lipoproteins (Morton and Greene, 2003; Swenson et al., 1988), or transfer lipids from lipoproteins to liposomes (Morton and Izem, 2014). We report here that JH binding by JHBP is reduced in the presence of DMPG liposomes (Figure 6), and that JHBP strongly interacts with these phospholipid membranes, as judged by its effect on TMA-DPH fluorescence anisotropy in DMPG liposomes (Figure 7). It is therefore tempting to speculate that lepidopteran JHBPs, with their single TULIP domain, could deliver their lipidic hormonal cargo upon docking to plasma membranes, through a mechanism analogous to lipid delivery at the phospholipid surface of lipoproteins by their vertebrate relatives CETP and PLTP. The fact that this effect seems modulated by anionic charge density (since liposomes composed of a mixture of DMPG and DMPC, a zwitterrionic phospholipid, had a much smaller effect on JH binding), suggests a primary involvement of electrostatic interactions. This is reminiscent of lipid transfer by CETP and PLTP, which is initiated by the electrostatic interaction of positively charged residues of CETP with negative charges (probably carried by phospholipids) at the lipoprotein surface (Desrumaux et al., 1998; Lagrost, 1994).

The data reported here are also similar to the findings on fatty acid binding proteins (FABPs), a family of small LTPs characterized by an antiparallel ß-barrel fold. Fatty-acid binding by Liver FABP (L-FABP), for example, shows a steep decline towards the acidic region, and is strongly inhibited with increased ionic strength, similarly to *Bm*JHBP (Stewart et al., 1998). Moreover, L-FABP binds to anionic phospholipid vesicles, and the mode of delivery of fatty acids to target membranes is thought to be collisional, rather than to depend on simple diffusion. It is believed to depend first on electrostatic interactions with anionic phospholipids at the membrane surface, leading to a conformational change inducing ligand release, but involves a subsequent membrane insertion or equivalent hydrophobic interactions (Corsico et al., 1998; Davies et al., 1998, 1999). Since we found evidence for both electrostatic and hydrophobic interactions with phospholipids (Figures 6 and 7), our data also suggest a collisional model of ligand release for *Bm*JHBP. It is then conceivable that key interactions stabilizing the α1 helix in the closed conformation, such as the hydrogen bonds between the α1 helix and the C terminus described by Suzuki and colleagues (Figure S1, (Suzuki et al., 2011)), may be destabilized as part of the release mechanism.

Further experiments will be required to examine if ligand release actually depends on a locally lower pH, or alternatively, if low pH *in vitro* only mimics a combination of electrostatic forces prevailing in the vicinity of target membranes *in vivo*. For example, ligand release on target membranes enriched in acidic phospholipids could be explained by the creation of a negative surface potential, leading to a local increase in proton concentration.

Collectively, the data presented here support the model of ligand release first envisioned for *G. mellonella* JHBP and *E. postvittana* Takeout 1 (Hamiaux et al., 2009; Kolodziejczyk et al., 2008)1, and described in detail for *B. mori* JHBP by Suzuki and colleagues (Suzuki et al., 2011), whereby JH is released by a movement of the α1 helix to the open conformation, and suggest that ligand release could be triggered by both electrostatic and hydrophobic interactions with the target membranes. These findings may be of general relevance for other JHBPs and Takeout proteins, since the structure of *G. mellonella* JHBP and *E. postvittana* Takeout 1 proteins are strikingly similar, presenting also an N terminal α1 helix followed by a loop possibly playing the role of a gatepost (Hamiaux et al., 2009; Kolodziejczyk et al., 2008; Suzuki et al., 2011), and because molecular simulations have suggested that ligand entry and release by *E. postvittana* Takeout 1 may occur in this region of the protein (Zhang et al., 2016). Ligand release from the other side of the protein may coexist with this mechanism, however, in the case of large ligands fitting in the continuous binding pocket of Takeout proteins (Hamiaux et al., 2009).

Figure Legends

Fig. 1. Ligand binding by lepidopteran JHBPs is reduced at acidic pH.

Binding of [^{3}H]-JH III by native *B. mori* JHBP (n*Bm*JHBP), recombinant *B. mori* JHBP (r*Bm*JHBP), and recombinant *M. sexta* JHBP (r*Ms*JHBP) was assayed by the Dextran Coated Charcoal (DCC) method **(A)** and dialysis assay **(B)**. To allow comparison, the highest percentage of bound [^{3}H]-JH III observed is set to 100% for each protein. The pH values inducing a 50% reduction in binding (pH_{50}) were determined from the curves in **(A)** and are respectively equal to 4.18, 4.67, 5.08 and 5.45 for r*Bm*JHBP, r*Ms*JHBP, n*Bm*JHBP and native *G. mellonella* JHBP (n*Gm*JHBP, data inferred and redrawn with permission from figure 7 in (Ozyhar and Kochman, 1987)). **(C, D)** The K_d values of r*Bm*JHBP for JH III at two different temperatures were determined by isothermal titration calorimetry (ITC). **(C)** Illustration of results of a typical ITC experiment, with 5µM r*Bm*JHBP and 70 µM JH III, at pH 7 and 20 °C: raw data (top), and integrated data (bottom). The arrow indicates the slope of the curve used to determinate K_d. **(D)** Summary of K_d determinations by ITC. *: p <0.05, Student's t test, unpaired, one-tailed, n = 3.

Fig. 2. Reversibility of the effect of low pH.
Recombinant *B. mori* JHBP (ca. $1.2 \cdot 10^{-7}$ M) was incubated with $2 \cdot 10^4$ dpm [^{3}H]-JH III for 2 h at pH 7 (black column), for 1 h at pH 7, then for 1 h at pH 4 after adjusting the pH (hatched column), or first for 1 h at pH 4, then for 1 h at pH 7 after adjusting the pH (white column). Initial incubations were done in 100 µL diluted McIlvaine buffer (1/10), and pH adjustment was obtained by addition of an equal volume of undiluted buffer at the desired pH. The percentage of bound hormone was determined with the DCC assay. ***: p < 0.001 Student's t test, unpaired, two-tailed, n = 3 (black and hatched columns) or n = 5 (white column).

Fig. 3. Near UV CD spectra of r*Bm*JHBP at different pH values.
Near UV CD spectra of r*Bm*JHBP were recorded between 320 and 250 nm. The spectra were recorded for a 10 µM r*Bm*JHBP solution in McIlvaine buffer with varying pH.

Fig. 4. Fluorescence emission spectra of r*Bm*JHBP.
(A) The spectra of a 10 µM protein solution were recorded after excitation at 295 nm before (solid line) and after 15 min equilibration with JH III at various concentrations. The measured intrinsic fluorescence is given in arbitrary units (A.U.) In **(B)**, the spectra were recorded for a 10 µM protein solution without ligand, in McIlvaine buffer at varying pH.

Fig. 5. Dissociation kinetics of JH III from JHBP.
To estimate the half-life ($t_{1/2}$) of the n*Bm*JHBP-JH III complex and the rate constant of dissociation (k_{off}), n*Bm*JHBP was first incubated in McIlvaine buffer at pH 7, 0 M NaCl with labelled hormone ([^{3}H]-JH III) to achieve equilibrium. At t_0, an equal volume of DCC slurry was added, allowing buffer change (0.6 M NaCl **(A)**, or pH 4 **(B)**), as well as quick and complete removal of unbound hormone (Fig. S8 (A)). DCC was next eliminated by centrifugation, after incubation for various periods of time. Since the amount of JHBP left in solution decreased only slowly with time, and was similar in the different conditions (Fig. S8 (B)), the radioactivity in the supernatant presumably reflects the release of [^{3}H]-JH III by JHBP. **(A)** Effect of high ionic strength. **(B)** Effect of pH. n = 3-6 for each time point. *** indicates P < 0.0001.

Fig. 6. Inhibition of binding of JH III to JHBP by model membranes. Binding of [^{3}H]-JH III by r*Bm*JHBP was assayed with a dialysis assay (see Material and Methods for details). The black column represents [^{3}H]-JH III bound to r*Bm*JHBP at equilibrium. Note that DMPG liposomes alone were also able to bind a significant, but smaller amount of [^{3}H]-JH III (white columns). DMPG/DMPC liposomes bind similar amounts of [^{3}H]-JH III (data not shown). When r*Bm*JHBP was incubated together with 40 µg or higher amounts of anionic liposomes, the total amount of bound [^{3}H]-JH III was significantly reduced (DMPG, striped columns) compared to the JHBP-only control, and was comparable to the amount bound by DMPG vesicles alone. In contrast, 600 µg of liposomes composed of a 1:1 ratio of DMPC and DMPG only slightly inhibited binding (DMPG/DMPC liposomes, grey columns). ***: p<0.0001**,** N=3-9, Student's t test, two-tailed.

Fig. 7. Steady-state fluorescence anisotropy of TMA-DPH in DMPG liposomes.

TMA-DPH was incubated in 1 mM Tris-HCl, pH 7.5 with DMPG liposomes alone, or with DMPG liposomes and r*Bm*JHBP, BSA or heat-denatured r*Bm*JHBP. Each curve represents the average of three replicates. Protein concentration was ~ 4 nM, and DMPG concentration was ~ 145 µM, thus the lipid:protein molar ratio was ~ 1:35000 (lipid:protein mass ratio ~ 1/1000).

Legends of supplementary figures

Supplementary figure S1. Crystal structure of *B. mori* holo- (A) and apo-JHBP (B).
(A) Juvenile hormone II (JH II, shown as balls and sticks) bound to JHBP (PDB id: 3AOS). The gate-forming amino-terminal α helix (α1) is shown in red, and the "gatepost" is highlighted in green. W38 is the only tryptophan residue of *B. mori* JHBP, and the main contributor to the JHBP fluorescence (Fig. 4). The residues in yellow are involved in direct hydrogen bonds that participate in keeping the α1 helix in its closed position. They are shown here only as examples of candidate bonds that may be disturbed at low pH. The closed conformation is further stabilized by polar interactions involving water molecules, as well as polar and hydrophobic interactions with JH II (Suzuki et al., 2011). **(B)** Apo-JHBP (PDB id: 3AOT). The arrow depicts the ca. 70 ° swing of the α1 helix allowing JH II release in the open conformation (Suzuki et al., 2011). The images were done with PyMOL 2.3.1.

Supplementary figure S2. Purification of native and recombinant JHBPs.
(A) Flow-chart for purification. The Coomassie stained gel at the bottom shows purified proteins used in this study. Purity is estimated to be greater than 95%. Note that both native and recombinant proteins migrate with apparent molecular weights around 30 kDa instead of the predicted molecular weight (~ 25 kDa). This electrophoretic behavior has been already noted in previous studies (see for example (Vermunt et al., 2001)). **(B)** Representative last purification step of recombinant *B. mori* JHBP (r*Bm*JHBP) on hydroxyapatite (Ceramic Hydroxyapatite Type I, BioRad). Bars represent concentrations of sodium phosphate used for elution, the doted line shows [^{3}H]-JH III binding capacity of each fraction. In the Coomassie stained gel at the bottom, stars indicate fractions pooled for experiments. On the X axis the names of collected fractions are shown. Start: starting material, FT: Flow Through, W: Wash, MW: Molecular weight markers (kDa).

Supplementary figure S3. Sequence of the cDNA encoding *B. mori* JHBP used in this study.
The first codon (GAT) of the mature protein (after the excision of the putative signal peptide predicted in (Vermunt et al., 2001) starts at position 7, and the 6 first nucleotides encode 2 residues added in this study for expression purposes (Met1, Gly2). We found 28 nucleotide differences in our strain (top sequence), when compared to the sequences published in (Vermunt et al., 2001) (bases in red). Among these base changes, 13 were synonymous, and the remaining 15 lead to a total of 10 amino acid substitutions. Three of these amino acid changes (highlighted in yellow) were also found by Vermunt and colleagues in an independent cDNA referred to as JHBP2. These variants presumably reflect the allelic variability of the different strains of silkworms used in the two studies.

Supplementary figure S4. Stability of JH III at various pHs.
(A) [^{3}H]-JH III (about 10000 dpm) was incubated for one hour at 20 °C in McIlvaine buffer, at various pH (3 replicates each), and analyzed by TLC. **(B)** The regions of interest of the silica plate (intact [^{3}H]-JH III and polar metabolites) were scraped off and radioactivity was counted. Student's t-test n = 3 *: p = 0.0086. Note that although there is a significantly higher degradation of [^{3}H]-JH III at pH 4, it cannot account for the decreased JH binding shown in Fig. 1. **(C)** Solubilization of [^{3}H]-JH III is not influenced by pH (n = 3).

Supplementary figure S5. Light scattering analysis of r*Bm*JHBP. The size and aggregation of r*Bm*JHBP (in McIlvaine buffer) was assayed with a Zetasizer light scattering device (Malvern, UK). The apparent radius of r*Bm*JHBP was not affected by pH (r = 2.56 ± 0.77 nm at pH 6.9; r = 2.49 ± 0.48 nm at pH 4.5). Some aggregation was evidenced at pH 4.5 (bottom left), but it represented a negligible fraction of the total protein. The % volume (right) reflects more accurately the relative

abundance in each size category, because intensity depends on light scattering, which is much greater for a large particle than for a small particle (the intensity of scattering is proportional to the sixth power of its diameter).

Supplementary figure S6. Effect of ionic strength on JH III binding by n*Bm*JHBP. JH III binding was measured using the DCC assay, in 10 mM Tris-HCl, pH 7, with NaCl concentrations as indicated.

Supplementary figure S7. Far-UV CD spectral analysis of r*Bm*JHBP at acidic and neutral pH.

Supplementary figure S8. Control experiments for analysis of ligand release by the DCC method. **(A)** Unbound labeled hormone ([^{3}H]-JH III) is efficiently removed by Dextran Coated Charcoal (DCC). [^{3}H]-JH III (about 100000 dpm) was incubated for 30 min at 20 °C, in the same buffers as those used for analysis of ligand release (Figure 5) and exposed for 20 s at 20 °C to DCC. After centrifugation, (30 s, ca.10000 g), the percentage of labelled hormone left in solution was measured by scintillation counting. Note that this short DCC treatment is sufficient to virtually eliminate all free [^{3}H]-JH III in the three different conditions. **(B)** Assessment of n*Bm*JHBP removal by DCC. To confirm that the apparent different half-lives of the complexes shown in Fig. 5 are not merely reflecting the differential binding of n*Bm*JHBP to charcoal in different buffers, n*Bm*JHBP was incubated in the same conditions as those used in Figure. 5. After 20 s (top) or 2 min (bottom) exposure to DCC, followed by a centrifugation to pellet charcoal (30 s, ca. 10000 g), the amount of protein remaining in solution was examined by SDS-PAGE and silver staining (Pierce). Note that there is no or little protein loss after 20 s exposure to DCC. Protein loss occurs after 2 min exposure, but appears similar in all three conditions. The asterisk indicates a 31 kDa MW marker.

Acknowledgments

This work was supported by INRA, CNRS, Université de Bourgogne Franche-Comté, and in its early stage by a grant from Région de Bourgogne to JPC.

References

Alva, V., Lupas, A.N., 2016. The TULIP superfamily of eukaryotic lipid-binding proteins as a mediator of lipid sensing and transport. Biochim. Biophys. Acta 1861, 913-923.

Barber, R.F., McKersie, B.D., Downer, R.G., Thompson, J.E., 1981. Perturbation of phospholipid membranes by juvenile hormone. Biochim. Biophys. Acta 643, 593-600.

Beamer, L.J., Carroll, S.F., Eisenberg, D., 1997. Crystal structure of human BPI and two bound phospholipids at 2.4 angstrom resolution. Science 276, 1861-1864.

Borenstain, V., Barenholz, Y., 1993. Characterization of liposomes and other lipid assemblies by multiprobe fluorescence polarization. Chem. Phys. Lipids 64, 117-127.

Butko, P., Cournoyer, M., Pusztai-Carey, M., Surewicz, W.K., 1994. Membrane interactions and surface hydrophobicity of *Bacillus thuringiensis* delta-endotoxin CryIC. FEBS Lett. 340, 89-92.

Charles, M.A., Kane, J.P., 2012. New molecular insights into CETP structure and function: a review. J. Lipid Res. 53, 1451-1458.

Chomczynski, P., Sacchi, N., 1987. Single-step method of RNA isolation by acid guanidinium thiocyanate-phenol-chloroform extraction. Anal. Biochem. 162, 156-159.

Corsico, B., Cistola, D.P., Frieden, C., Storch, J., 1998. The helical domain of intestinal fatty acid binding protein is critical for collisional transfer of fatty acids to phospholipid membranes. Proc. Natl. Acad. Sci. U.S.A. 95, 12174-12178.

Davies, J.K., Thumser, A.E., Wilton, D.C., 1998. Liver fatty acid binding protein (FABP) binds to anionic phospholipid vesicles with release of ligand. Biochem. Soc. Trans. 26, S238.

Davies, J.K., Thumser, A.E., Wilton, D.C., 1999. Binding of recombinant rat liver fatty acid-binding protein to small anionic phospholipid vesicles results in ligand release: a model for interfacial binding and fatty acid targeting. Biochemistry 38, 16932-16940.

Desrumaux, C., Athias, A., Masson, D., Gambert, P., Lallemant, C., Lagrost, L., 1998. Influence of the electrostatic charge of lipoprotein particles on the activity of the human plasma phospholipid transfer protein. J. Lipid Res. 39, 131-142.

Elving, P.J., Markowitz, J.M., Rosenthal, I., 1956. Preparation of buffer systems of constant ionic strength. Anal. Chem. 28, 1179-1180.

Fujikawa, K., Seno, K., Ozaki, M., 2006. A novel Takeout-like protein expressed in the taste and olfactory organs of the blowfly, *Phormia regina*. FEBS J. 273, 4311-4321.

Galikova, M., Flatt, T., 2010. Dietary restriction and other lifespan extending pathways converge at the activation of the downstream effector takeout. Aging (Albany NY) 2, 387-389.

Gasymov, O.K., Abduragimov, A.R., Yusifov, T.N., Glasgow, B.J., 2004. Interstrand loops CD and EF act as pH-dependent gates to regulate fatty acid ligand binding in tear lipocalin. Biochemistry 43, 12894-12904.

Goodman, W.G., 1990. Biosynthesis, Titer Regulation and Transport of Juvenile Hormones., in: Gupta, A.P. (Ed.), Morphogenetic Hormones of Arthropods. Rutgers University Press, New Brunswick and London, pp. 83-124.

Goodman, W.G., Bollenbacher, W.E., Zvenko, H.L., Gilbert, L.I., 1976. The Juvenile Hormones, Proceedings of an International Symposium on the Chemistry, Metabolism, and Modes of Action of the Juvenile Hormones of Insects. Plenum Press, New York, Lake Geneva, Wisconsin, pp. 75-95.

Goodman, W.G., Cusson, M., 2012. The juvenile hormones., in: Gilbert, L.I. (Ed.), Insect Endocrinology. Academic Press, New York, pp. 310-365.

Hamiaux, C., Basten, L., Greenwood, D.R., Baker, E.N., Newcomb, R.D., 2013. Ligand promiscuity within the internal cavity of *Epiphyas postvittana* Takeout 1 protein. J. Struct. Biol. 182, 259-263.

Hamiaux, C., Stanley, D., Greenwood, D.R., Baker, E.N., Newcomb, R.D., 2009. Crystal structure of *Epiphyas postvittana* Takeout 1 with bound ubiquinone supports a role as ligand carriers for Takeout proteins in insects. J. Biol. Chem. 284, 3496-3503.

Harrison, S.C., 2015. Viral membrane fusion. Virology 479-480, 498-507.

Hellmann, N., Schneider, D., 2019. Hands on: using tryptophan fluorescence spectroscopy to study protein structure. Methods Mol. Biol. 1958, 379-401.

Horst, R., Damberger, F., Luginbuhl, P., Guntert, P., Peng, G., Nikonova, L., Leal, W.S., Wuthrich, K., 2001. NMR structure reveals intramolecular regulation mechanism for pheromone binding and release. Proc. Natl. Acad. Sci. U.S.A. 98, 14374-14379.

Jiang, J.X., London, E., 1990. Involvement of denaturation-like changes in *Pseudomonas* exotoxin a hydrophobicity and membrane penetration determined by characterization of pH and thermal transitions. Roles of two distinct conformationally altered states. J. Biol. Chem. 265, 8636-8641.
Jindra, M., Belles, X., Shinoda, T., 2015. Molecular basis of juvenile hormone signaling. Curr. Opin. Insect Sci. 11, 39-46.
Koeppe, J.K., Kovalick, G.E., 1986. Juvenile Hormone-Binding Proteins, in: Litwack, G. (Ed.), Biochemical Actions of Hormones. Academic Press, New York, pp. 265-303.
Kolodziejczyk, R., Bujacz, G., Jakob, M., Ozyhar, A., Jaskolski, M., Kochman, M., 2008. Insect juvenile hormone binding protein shows ancestral fold present in human lipid-binding proteins. J. Mol. Biol. 377, 870-881.
Kolodziejczyk, R., Dobryszycki, P., Ozyhar, A., Kochman, M., 2001. Two disulphide bridges are present in juvenile hormone binding protein from *Galleria mellonella*. Acta Biochim. Pol. 48, 917-920.
Kramer, K.J., Sanburg, L.L., Kezdy, F.J., Law, J.H., 1974. The juvenile hormone binding protein in the hemolymph of *Manduca sexta* Johannson (*Lepidoptera: Sphingidae*). Proc. Natl. Acad. Sci. U.S.A. 71, 493-497.
Krzyzanowska, D., Lisowski, M., Kochman, M., 1998. UV-difference and CD spectroscopy studies on juvenile hormone binding to its carrier protein. J. Pept. Res. 51, 96-102.
Kurata, K., Nakamura, M., Okuda, T., Hirano, H., Shinbo, H., 1994. Purification and characterization of a juvenile hormone binding protein from hemolymph of the silkworm, *Bombyx mori*. Comp. Biochem. Physiol. B Biochem. Mol. Biol. 109, 105-114.
Lagrost, L., 1994. Regulation of cholesteryl ester transfer protein (CETP) activity: review of in vitro and in vivo studies. Biochim. Biophys. Acta 1215, 209-236.
Lamy-Freund, M.T., Riske, K.A., 2003. The peculiar thermo-structural behavior of the anionic lipid DMPG. Chem. Phys. Lipids 122, 19-32.
Lauer, M.E., Graff-Meyer, A., Rufer, A.C., Maugeais, C., von der Mark, E., Matile, H., D'Arcy, B., Magg, C., Ringler, P., Muller, S.A., Scherer, S., Dernick, G., Thoma, R., Hennig, M., Niesor, E.J., Stahlberg, H., 2016. Cholesteryl ester transfer between lipoproteins does not require a ternary tunnel complex with CETP. J. Struct. Biol. 194, 191-198.
Lazareva, A.A., Roman, G., Mattox, W., Hardin, P.E., Dauwalder, B., 2007. A role for the adult fat body in *Drosophila* male courtship behavior. PLoS Genet. 3, e16.
London, E., 1992. Diphtheria toxin: membrane interaction and membrane translocation. Biochim. Biophys. Acta 1113, 25-51.
Masson, D., Jiang, X.C., Lagrost, L., Tall, A.R., 2009. The role of plasma lipid transfer proteins in lipoprotein metabolism and atherogenesis. J. Lipid Res. 50 Suppl, S201-206.
McIlvaine, T.C., 1921. A buffer solution for colorimetric comparison. J. Biol. Chem. 49, 183-186.
Menestrina, G., Forti, S., Gambale, F., 1989. Interaction of tetanus toxin with lipid vesicles. Effects of pH, surface charge, and transmembrane potential on the kinetics of channel formation. Biophys. J. 55, 393-405.
Meunier, N., Belgacem, Y.H., Martin, J.R., 2007. Regulation of feeding behaviour and locomotor activity by Takeout in *Drosophila*. J. Exp. Biol. 210, 1424-1434.
Morton, R.E., Greene, D.J., 2003. The surface cholesteryl ester content of donor and acceptor particles regulates CETP: a liposome-based approach to assess the substrate properties of lipoproteins. J. Lipid Res. 44, 1364-1372.
Morton, R.E., Izem, L., 2014. Cholesteryl ester transfer proteins from different species do not have equivalent activities. J. Lipid Res. 55, 258-265.
Ozyhar, A., Kochman, M., 1987. Juvenile-hormone-binding protein from the hemolymph of *Galleria mellonella* (L). Isolation and characterization. Eur. J. Biochem. 162, 675-682.
Park, Y.C., Tesch, M.J., Toong, Y.C., Goodman, W.G., 1993. Affinity purification and binding analysis of the hemolymph juvenile hormone binding protein from *Manduca sexta.* Biochemistry 32, 7909-7915.
Prendergast, F.G., Haugland, R.P., Callahan, P.J., 1981. 1-[4-(Trimethylamino)phenyl]-6-phenylhexa-1,3,5-triene: synthesis, fluorescence properties, and use as a fluorescence probe of lipid bilayers. Biochemistry 20, 7333-7338.

Ptitsyn, O.B., Zanotti, G., Denesyuk, A.L., Bychkova, V.E., 1993. Mechanism of pH-induced release of retinol from retinol-binding protein. FEBS Lett. 317, 181-184.
Qiu, X., Mistry, A., Ammirati, M.J., Chrunyk, B.A., Clark, R.W., Cong, Y., Culp, J.S., Danley, D.E., Freeman, T.B., Geoghegan, K.F., Griffor, M.C., Hawrylik, S.J., Hayward, C.M., Hensley, P., Hoth, L.R., Karam, G.A., Lira, M.E., Lloyd, D.B., McGrath, K.M., Stutzman-Engwall, K.J., Subashi, A.K., Subashi, T.A., Thompson, J.F., Wang, I.K., Zhao, H., Seddon, A.P., 2007. Crystal structure of cholesteryl ester transfer protein reveals a long tunnel and four bound lipid molecules. Nat .Struct. Mol. Biol. 14, 106-113.
Royer, C.A., 2006. Probing protein folding and conformational transitions with fluorescence. Chem Rev 106, 1769-1784.
Sarov-Blat, L., So, W.V., Liu, L., Rosbash, M., 2000. The *Drosophila* Takeout gene is a novel molecular link between circadian rhythms and feeding behavior. Cell 101, 647-656.
Stewart, J.M., Dewling, V.F., Wright, T.G., 1998. Fatty acid binding to rat liver fatty acid-binding protein is modulated by early glycolytic intermediates. Biochim. Biophys. Acta 1391, 1-6.
Suzuki, R., Fujimoto, Z., Shiotsuki, T., Tsuchiya, W., Momma, M., Tase, A., Miyazawa, M., Yamazaki, T., 2011. Structural mechanism of JH delivery in hemolymph by JHBP of silkworm, *Bombyx mori*. Sci. Rep. 1, 133.
Swenson, T.L., Brocia, R.W., Tall, A.R., 1988. Plasma cholesteryl ester transfer protein has binding sites for neutral lipids and phospholipids. J. Biol. Chem. 263, 5150-5157.
Touhara, K., Lerro, K.A., Bonning, B.C., Hammock, B.D., Prestwich, G.D., 1993. Ligand binding by a recombinant insect juvenile hormone binding protein. Biochemistry 32, 2068-2075.
Tzotzas, T., Desrumaux, C., Lagrost, L., 2009. Plasma phospholipid transfer protein (PLTP): review of an emerging cardiometabolic risk factor. Obes. Rev. 10, 403-411.
Vega, S., Abian, O., Velazquez-Campoy, A., 2016. On the link between conformational changes, ligand binding and heat capacity. Biochim. Biophys. Acta 1860, 868-878.
Vermunt, A.M., Kamimura, M., Hirai, M., Kiuchi, M., Shiotsuki, T., 2001. The juvenile hormone binding protein of silkworm haemolymph: gene and functional analysis. Insect Mol. Biol. 10, 147-154.
Wieczorek, E., Kochman, M., 1991. Conformational change of the haemolymph juvenile-hormone-binding protein from *Galleria mellonella* (L). Eur. J. Biochem. 201, 347-353.
Wojtasek, H., Leal, W.S., 1999. Conformational change in the pheromone-binding protein from *Bombyx mori* induced by pH and by interaction with membranes. J. Biol. Chem. 274, 30950-30956.
Wong, L.H., Levine, T.P., 2017. Tubular lipid binding proteins (TULIPs) growing everywhere. Biochim. Biophys. Acta Mol. Cell. Res. 1864, 1439-1449.
Yoshizawa, Y., Sato, R., Tsuchihara, K., Ozaki, K., Mita, K., Asaoka, K., Taniai, K., 2011. Ligand carrier protein genes expressed in larval chemosensory organs of *Bombyx mori*. Insect Biochem. Mol. Biol. 41, 545-562.
Zhang, H., Yu, H., Zhao, X., Liu, X., Feng, X., Huang, X., 2016. Investigations of Takeout proteins' ligand binding and release mechanism using molecular dynamics simulation. J. Biomol. Struct. Dyn. 35, 1464-1473.
Zhang, L., Yan, F., Zhang, S., Lei, D., Charles, M.A., Cavigiolio, G., Oda, M., Krauss, R.M., Weisgraber, K.H., Rye, K.A., Pownall, H.J., Qiu, X., Ren, G., 2012. Structural basis of transfer between lipoproteins by cholesteryl ester transfer protein. Nat. Chem. Biol. 8, 342-349.

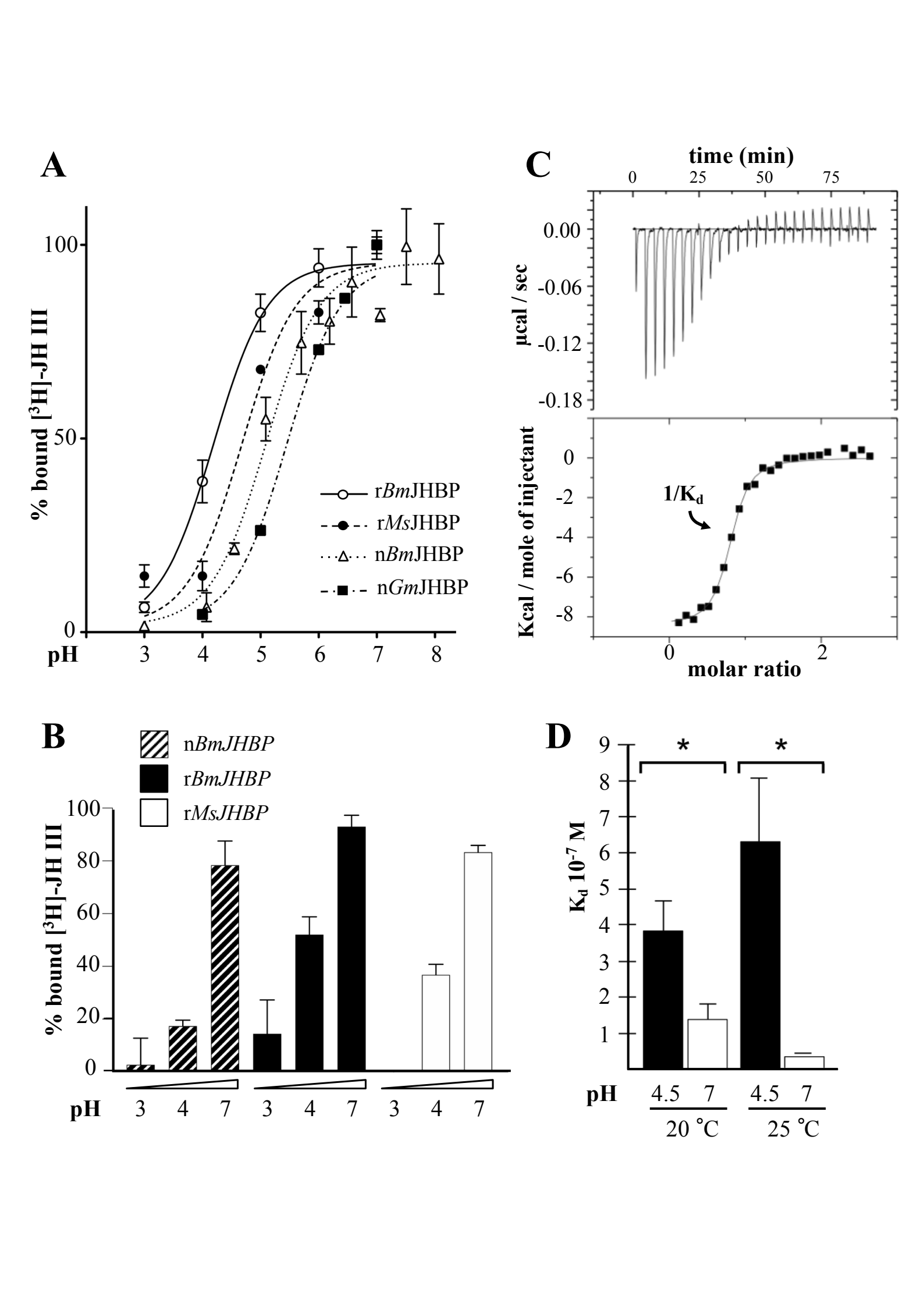
A
% bound [3H]-JH III
100
50
0
pH
3
4
5
6
7
8
rBmJHBP
rMsJHBP
nBmJHBP
nGmJHBP
C
time (min)
0
25
50
75
µcal / sec
0.00
-0.06
-0.12
-0.18
Kcal / mole of injectant
0
-2
-4
-6
-8
1/Kd
0
2
molar ratio
B
nBmJHBP
rBmJHBP
rMsJHBP
% bound [3H]-JH III
100
80
60
40
20
0
pH
3
4
7
3
4
7
3
4
7
D
Kd 10-7 M
9
8
7
6
5
4
3
2
1
*
*
pH
4.5
7
4.5
7
20 ˚C
25 ˚C

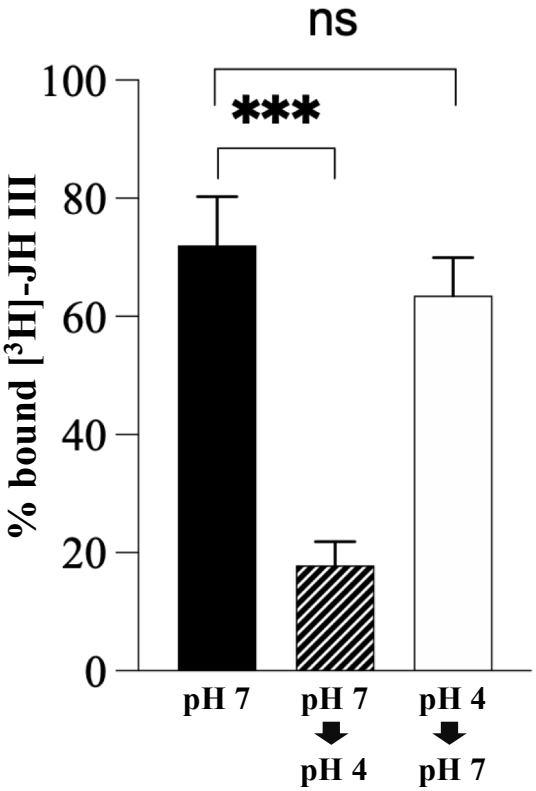
ns
***
100
80
60
40
20
0
% bound [3H]-JH III
pH 7
pH 7
pH 4
pH 4
pH 7

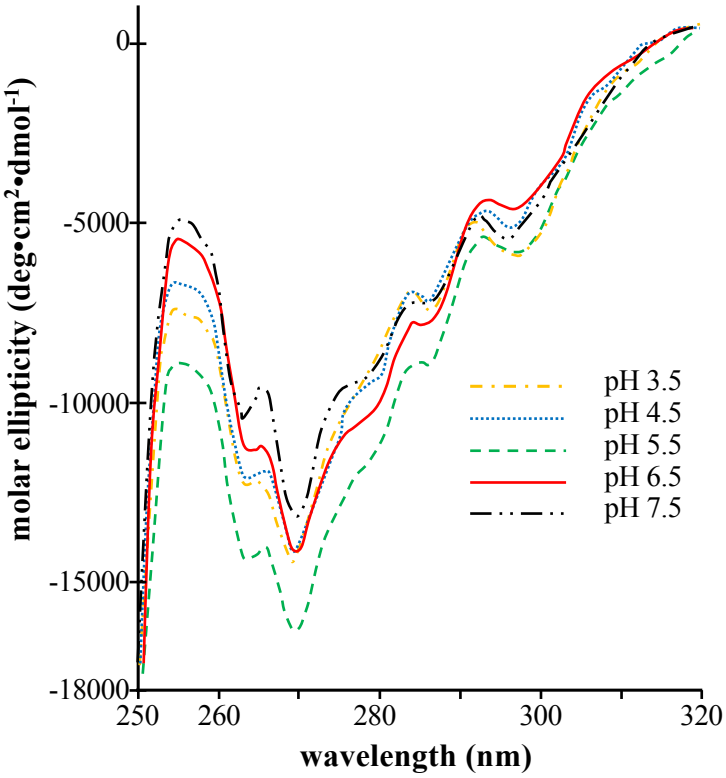
0
-5000
-10000
-15000
-18000
molar ellipticity (deg•cm²•dmol⁻¹)
250
260
280
300
320
wavelength (nm)
pH 3.5
pH 4.5
pH 5.5
pH 6.5
pH 7.5

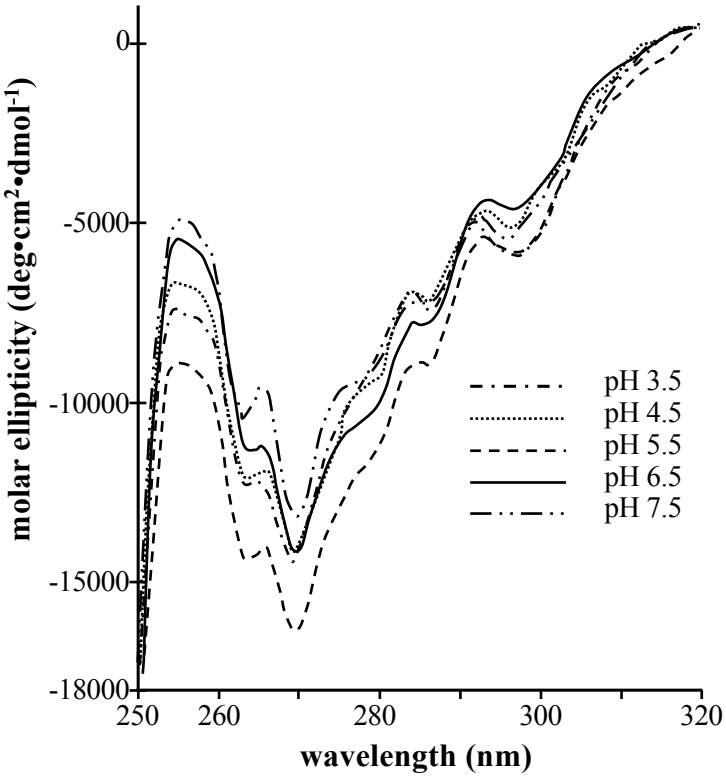
0
-5000
-10000
-15000
-18000
250
260
280
300
320
molar ellipticity (deg•cm²•dmol⁻¹)
wavelength (nm)
pH 3.5
pH 4.5
pH 5.5
pH 6.5
pH 7.5

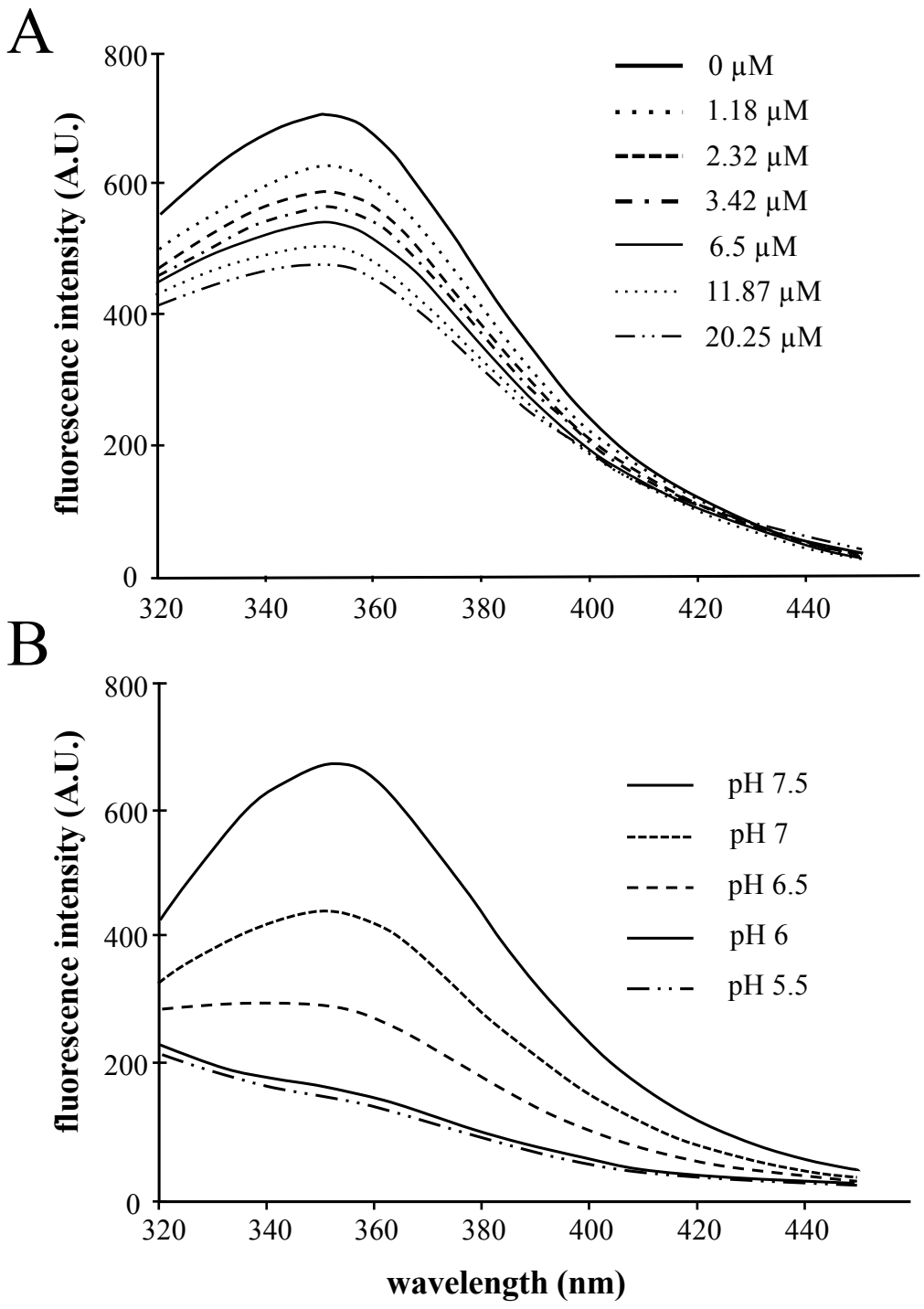
A
800
600
400
200
0
fluorescence intensity (A.U.)
320
340
360
380
400
420
440
0 µM
1.18 µM
2.32 µM
3.42 µM
6.5 µM
11.87 µM
20.25 µM
B
800
600
400
200
0
fluorescence intensity (A.U.)
320
340
360
380
400
420
440
wavelength (nm)
pH 7.5
pH 7
pH 6.5
pH 6
pH 5.5

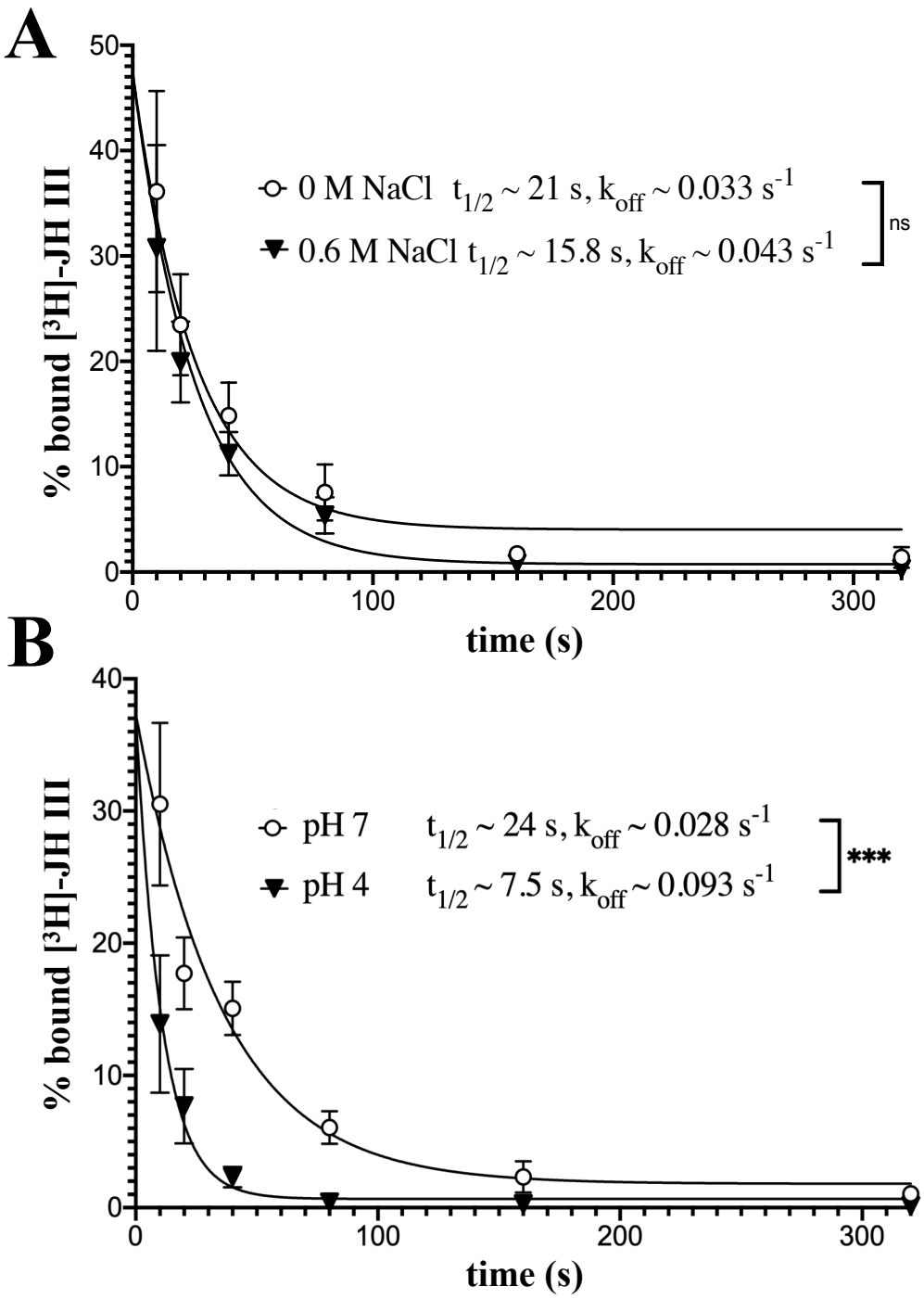
A
% bound [3H]-JH III
0 M NaCl t1/2 ~ 21 s, koff ~ 0.033 s-1
0.6 M NaCl t1/2 ~ 15.8 s, koff ~ 0.043 s-1
ns
time (s)
B
% bound [3H]-JH III
pH 7 t1/2 ~ 24 s, koff ~ 0.028 s-1
pH 4 t1/2 ~ 7.5 s, koff ~ 0.093 s-1
***
time (s)

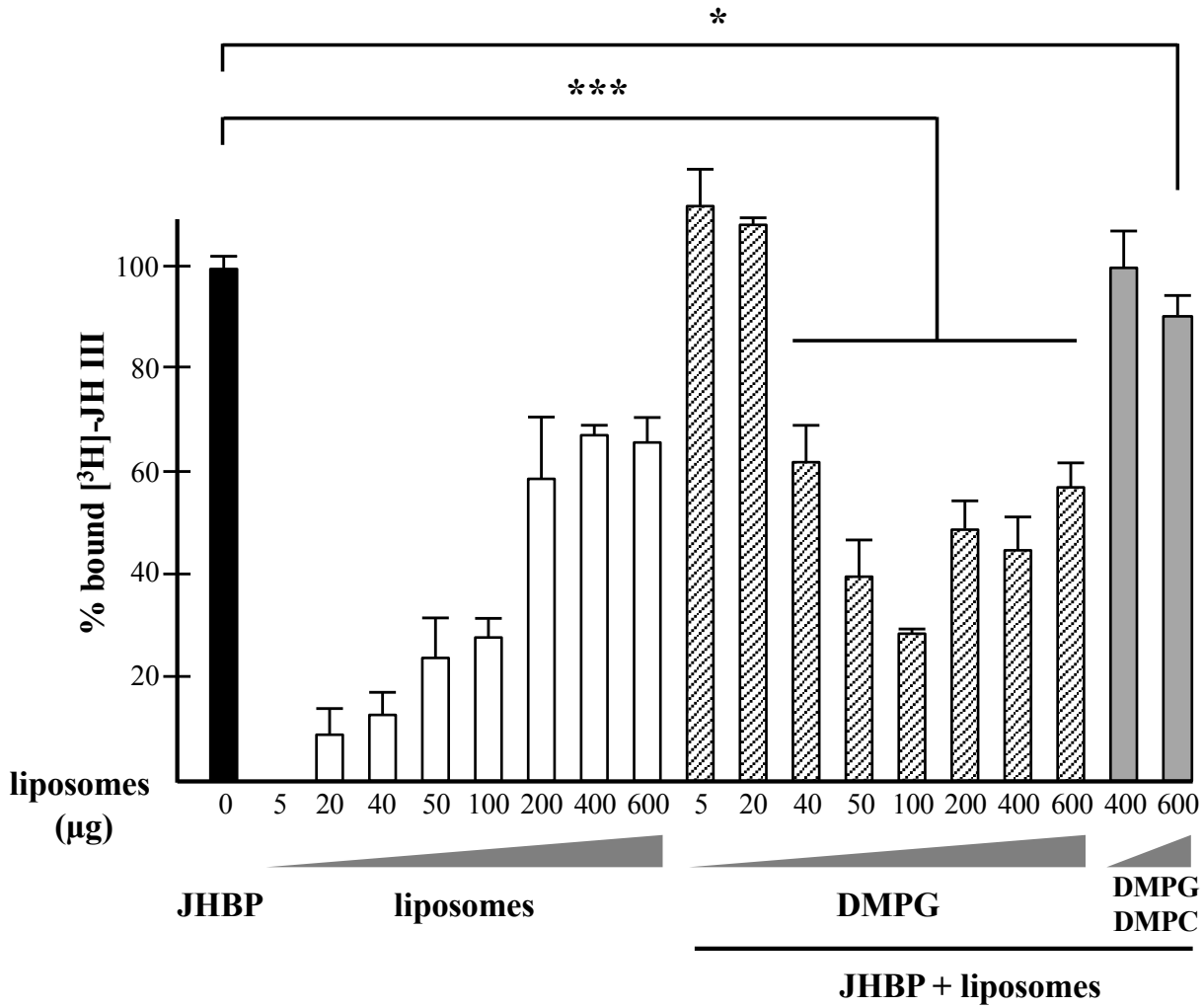
*
***
% bound [3H]-JH III
100
80
60
40
20
liposomes (µg)
0 5 20 40 50 100 200 400 600 5 20 40 50 100 200 400 600 400 600
JHBP
liposomes
DMPG
DMPG DMPC
JHBP + liposomes

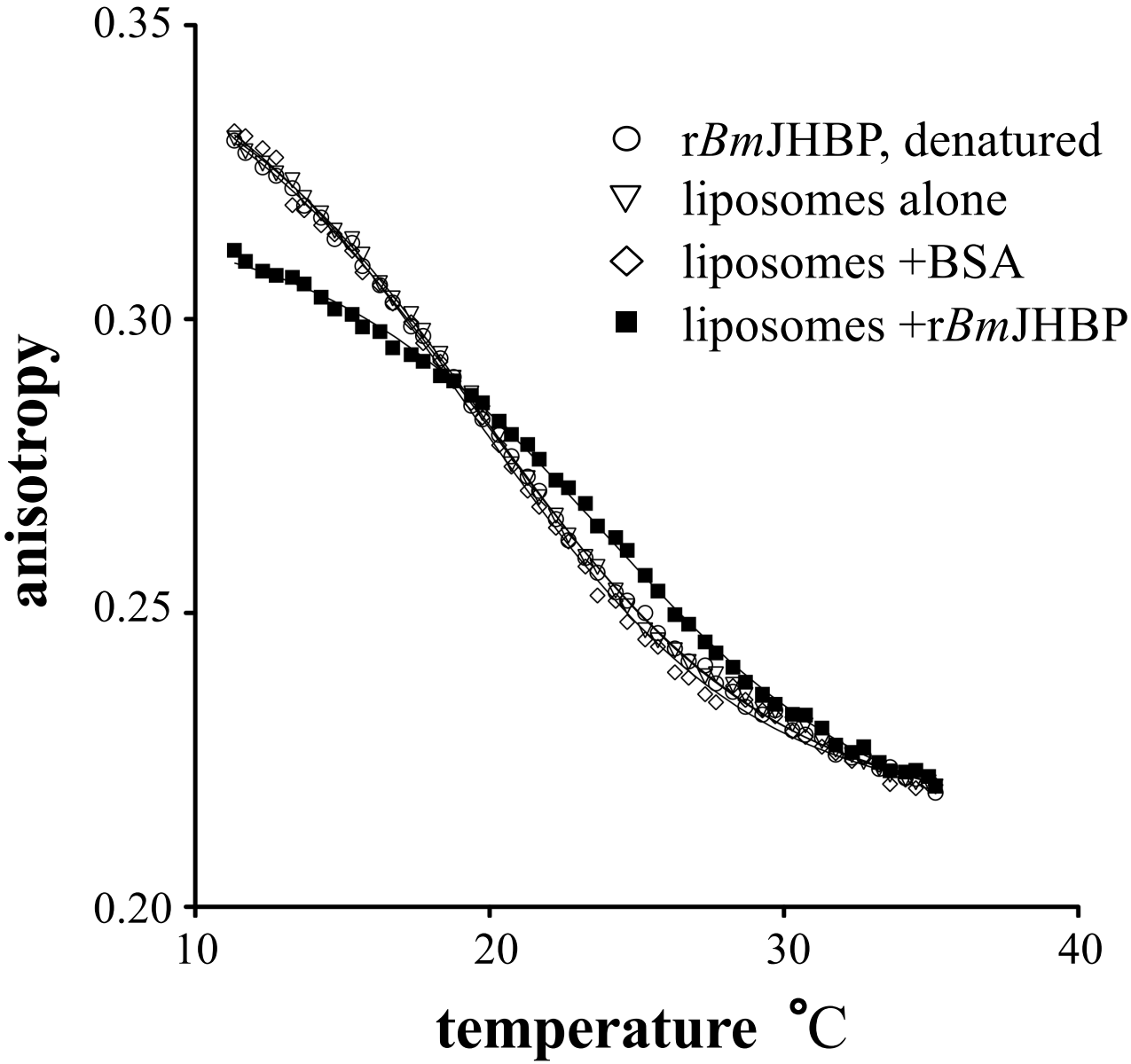
0.35
0.30
0.25
0.20
anisotropy
10
20
30
40
temperature ℃
r*Bm*JHBP, denatured
liposomes alone
liposomes +BSA
liposomes +r*Bm*JHBP

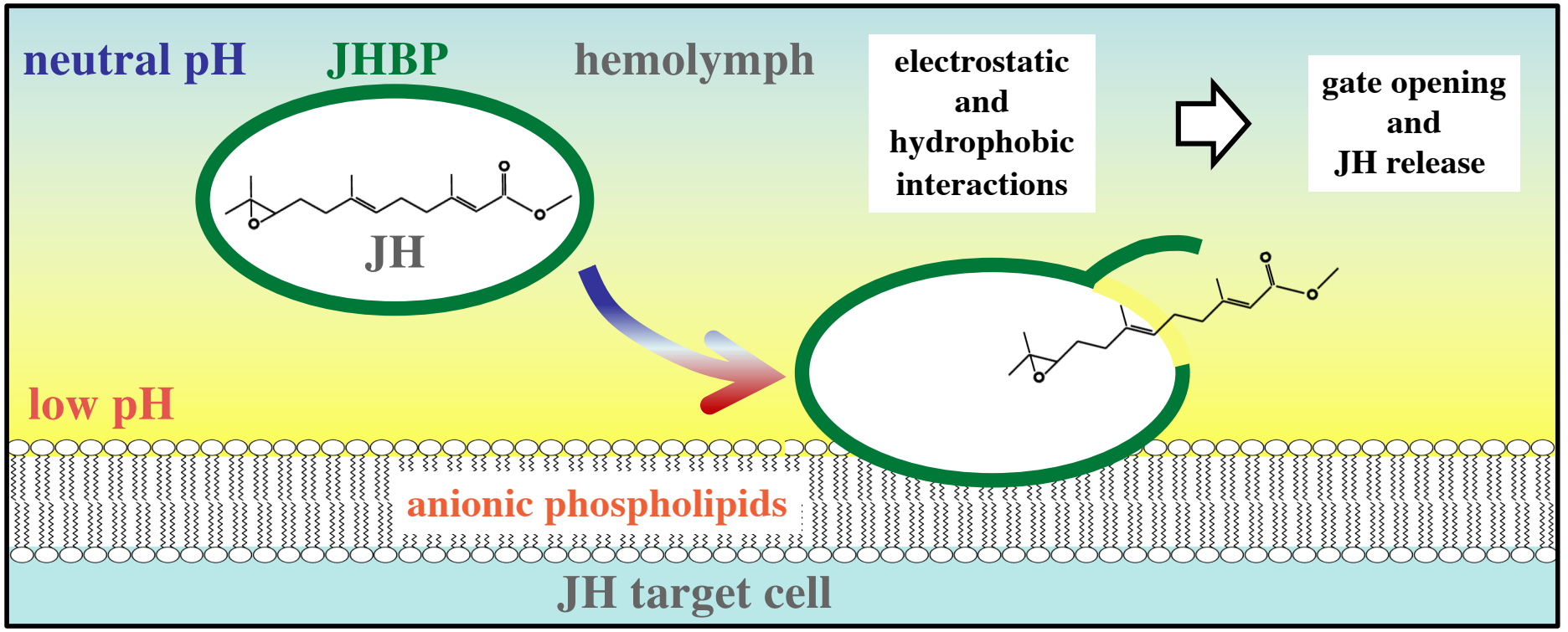
neutral pH
JHBP
hemolymph
JH
electrostatic
and
hydrophobic
interactions
gate opening
and
JH release
low pH
anionic phospholipids
JH target cell